Available online at www.sciencedirect.com
ScienceDirect
Journal of Nuclear Materials 363–365 (2007) 1016–1020
journal of nuclear materials
www.elsevier.com/locate/jnucmat

Positive sheath behaviour in low pressure Argon plasma

L. Schiesko *, M. Carrère, G. Cartry, J.M. Layet

Plasma Surface, PIIM, UMR 6633, Université de Provence – CNRS, Centre scientifique de Saint Jérôme, case 241, 13397 Marseille cedex 20, France

Abstract

We measure positive ions by means of a Hiden mass spectrometer (EQP 300) in a helicon discharge. Our helicon 'PHISIS' (plasma helicon to irradiate surfaces in situ) is used at low injected RF power, in a capacitive regime. A copper sample is centred in the expanding chamber, 40 mm away from the mass spectrometer nozzle. We measure ion energy distribution function (IEDF) for different sample positive bias. We show the absence of ions having energies corresponding to the full acceleration inside the positive sheath. We attribute this effect to secondary electron emission induced by electrons extracted from the plasma to the sample surface, which changes the potential profile and neutralise low energy ions created close to the sample surface (radiative recombination).

PACS: 52.40.Hf; 79.20.Hx

Keywords: Argon; Plasma boundary; Electron emission; Plasma facing components; Plasma sheath phenomena

1. Introduction

Since David Bohm, ion and electron dynamics in the sheath have been widely studied by physicists and mathematicians. Sheath acts as the transition between plasma and surface, and is therefore a crucial element in many fields of plasma applications like tokamak (ITER), etching [1], plasma immersion for ion implantation (PIII) [2,3]. If dynamics of the sheath is dominated by one specie (electron or ion) it is called space charge limited or Child–Langmuir (CL) sheath. The corresponding Child–Langmuir law fixes condition between current, voltage and size of the sheath. Mathematician Degond published many work about this law since 1990 [4]. This law is used in many fields of physics [5–7], for example in semiconductor physics [8,9]. Recent studies focus on 2D or time dependent behaviour [5,10]. In this paper we study plasma surface physics by measuring ion flux coming from a positive Child–Langmuir transition between plasma and a copper sample. At low pressure the electron current which is space charge limited creates few ionization inside the positive sheath. Each created ion returns towards plasma, and reaches mass spectrometer with an energy $\varepsilon = e\phi$ corresponding to the local potential ϕ at which it has been created. Ion energy distribution function (IEDF) measurements give information on ionization inside the sheath and on interaction of electrons with sample surface.

* Corresponding author.
E-mail address: loic.schiesko@up.univ-mrs.fr (L. Schiesko).

0022-3115/$ - see front matter
doi:10.1016/j.jnucmat.2007.01.137

In particular, it shows that a kind of electron gas exists close to the sample positively biased. The aim of this paper is to understand positive sheath dynamics. Indeed positively biased samples could be used as plasma surface interaction diagnostic in tokamaks. X-rays emitted by bombarded samples could be analysed to determine surface modifications [11] (appearance potential spectroscopy technique, APS). In the present paper we study a positively biased copper sample in an argon plasma for sake of simplicity. This paper is divided in three parts: first we present our experimental set up, then we describe IEDF measurements and finally we discuss on IEDF shapes.

2. Experimental set-up

The experimental set-up is described in [12]. It is an helicon reactor, (PHISIS, plasma helicon to irradiate surfaces in situ) which consists of an upper source chamber and a lower diffusion chamber. The source has been designed by ANU (Canberra University), it is a 150 mm diameter, 200 mm long Pyrex cylinder, surrounded by a double loop antenna (Boswell antenna). The matching box is an L type with a 0–2000 pF tune capacitor and a 0–1000 pF load capacitor and is controlled manually. The total volume of the reactor is around 10 l [12]. A base pressure lower than 10^{-5} Pa (penning gauge limit) is achieved in the chamber by mean of a 150 l/s turbomolecular pump. During plasma operation, the pressure is controlled by a Baratron gauge.

We use a Langmuir probe from Scientific System (Smart Probe) to measure electronic density and temperature.

Our mass spectrometer is a Hiden EQP 300: it comprises an extraction orifice (diameter: 35 μm), which can be biased to attract positive or negative ions, an ionisation chamber for neutral analysis (residual gas analysis: RGA), some collimating lenses, a 45° electrostatic energy analyser, a quadruple mass filter and a secondary electron multiplier. It thus allows us to analyse the ion energy distribution function (IEDF) for positive and negative ions and the RGA is useful for controlling gas purity. Our spectrometer is differentially pumped to below 10^{-6} Pa by means of a turbomolecular pump (70 l/s) followed by a primary pump. It is horizontally inserted in the spherical expanding plasma chamber which places the extraction orifice 20 mm off axis, in the centre of the stainless steel sphere.

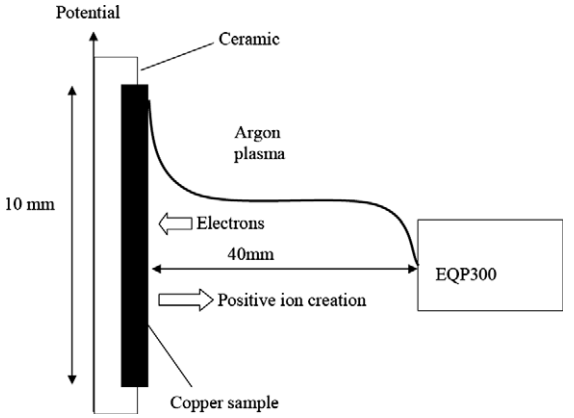

Fig. 1. Sketch of the experimental set-up: sample, plasma and EQP nozzle.

The sample holder places our 1 cm^2 copper sample 40 mm away from the mass spectrometer nozzle. Except for one face, in front of the spectrometer, it is totally covered by a ceramic insulator. The sample could be polarised from 1 to −1 kV, but here it was biased from 70 to 210 V. Fig. 1 sketches the sample, the plasma and the EQP nozzle.

Measurements were made for an injected power of 200 W (capacitive regime), without magnetic confinement, for argon gas. Results for two pressures are presented in this paper, 5×10^{-2} and 10^{-1} Pa. Plasma potential (potential between plasma and ground), as measured by Langmuir probe, is 51 V at 5×10^{-2} Pa and 36 V at 10^{-1} Pa. In order to keep a constant ion transmission function inside the mass spectrometer, control parameters such as acquisition time and lens potentials were kept constant for all measurements at one pressure. Moreover, in order to always scan the same energy window (around 20 V), the whole mass spectrometer was floating at a potential slightly lower than the sample bias.

3. Measurements

In the sheath, ions are created by the electrons extracted at plasma boundary with thermal velocity and continuously accelerated. Of course charged particles are in equilibrium with potential and Poisson equation is always valid. We assume that CL law is obtained between plasma and sample. Indeed, due to the huge difference between ion density and electron density (ratio $\sim 10^6$) in the sheath, sheath potential curvature is mainly governed by electrons. The sample is positively biased, electrons from plasma are attracted and

bombard the sample, and ions are created from the background neutral Ar population by these incident electrons in the sheath. Once created, ions are accelerated by the electric field in the opposite direction and collected by mass spectrometer. Calculus of relevant mean free path, such charge transfer and momentum transfer for Ar^+–Ar collisions [13] leads to an order of magnitude of 10 cm for these reactions. Ion–ion collisions rates are too low to be considered. Therefore ions do not suffer any collision during their acceleration from the positive sheath to mass spectrometer, and their measured energy ε corresponds to the potential at which they are created ($\varepsilon = e\phi$). Electronic ionization [14,15] mean free path is about two orders of magnitude more that ion mean free path. Thus, very few ionization occurs inside the sheath, explaining low IEDF signal to noise ratio.

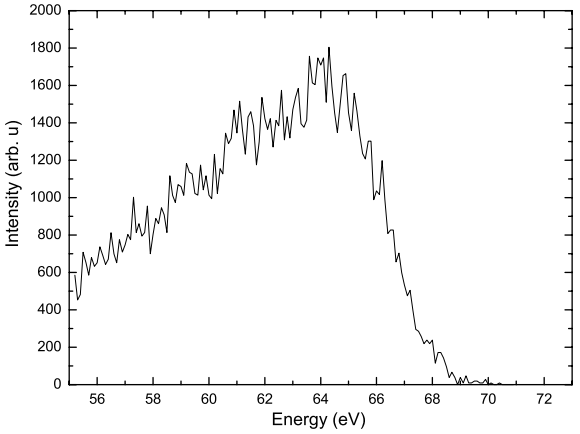

Fig. 2. Ion energy distribution function (IEDF) obtained in argon plasma at 0.05 Pa, a sample bias of 70 V and 200 W of injected power.

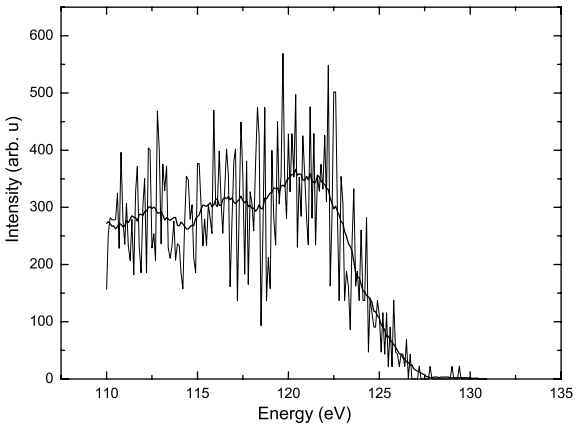

Fig. 3. Ion energy distribution function (IEDF) obtained in argon plasma at 0.1 Pa, a sample bias of 130 V and 200 W of injected power.

Figs. 2 and 3 show typical IEDF obtained at two different sample bias, 70 V and 130 V. One can see in Figs. 2 and 3 that no ion are detected at the full acceleration energy ($\varepsilon = e\phi_0$ where ϕ_0 is the sample surface). We call the difference between the highest ion energy of the IEDF and sample potential, the cut off for sake of simplicity, despite it is rather a decrease of the signal below detection limit. In Fig. 2 for example the cut off is around 1 eV. Cut off is due to a small area in front of the surface sample that looks depleted of ions.

4. Discussion

Electrons coming from plasma and accelerated inside the sheath strike the surface and induce secondary emission. Our hypothesis is that the cut off is caused by secondary electrons emitted by the sample. First, the increase of electron density near the sample could locally lower the potential (this effect can be seen as a shielding effect) and reduce ion energy. Second, the radiative recombination process could be increased by the presence of low energy electrons emitted by the surface, and could reduce ion density close to surface. Finally both effects could occur simultaneously.

In Fig. 4 we present a synthesis of cut off measurements. The curves have been drawn for two pressures (5×10^{-2} Pa and 10^{-1} Pa). The bias potential applied to the sample varies from 70 to 210 V for each pressure. The cut off changes with pressure and bias.

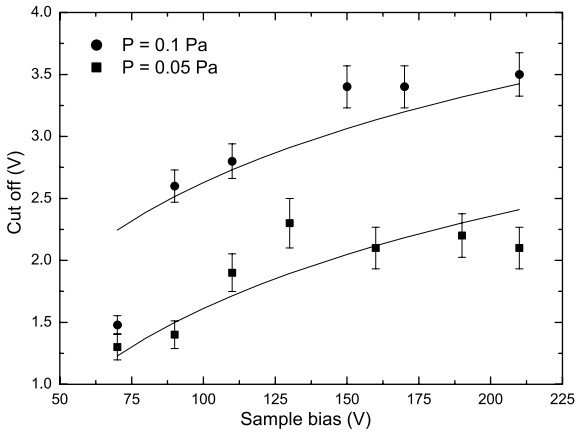

Fig. 4. Cut off versus sample bias for 200 W argon plasma. Squares: 0.05 Pa. Circles: 0.1 Pa. Lines are a logarithmic fit of experimental results.

We assume that secondary electrons, emitted from the surface at a temperature T_{es}, are in Boltzmann equilibrium with the potential:

$$n_{es}(x) = n_{e0} e^{\left(\frac{\phi(x)-\phi_0}{k_B T_{es}}\right)}, \quad (1)$$

with $n_{es}(x)$ the secondary electronic density, n_{e0} the secondary electronic density at the sample surface, e the electronic charge, $\phi(x)$ the potential, ϕ_0 the sample bias, k_B the Boltzmann constant and T_{es} the secondary electronic temperature.

If we assume that close to surface secondary electron density is much higher than primary electron density, potential is then determined by secondary electrons only. As secondary electron density exponentially decreases, potential also has an exponential curvature (this can be checked by integrating the Poisson equation including only secondary electrons and by expanding to the first order in a Taylor series the exponential function for $e(\phi - \phi_0) \ll k_B T_{es}$). Therefore the potential drops drastically close to the sample, on a distance too short to observe a significant ionization signal. This fast variation ends as soon as the primary electron density is no more negligible compared to the secondary electron density. Assuming n_{esmin} is the density of secondary electrons below which the primary electron density is no more negligible, the following calculus permits to understand the behaviour of the cut off with the applied bias:

$$n(x) = n_{esmin} \Longleftrightarrow n_{e0} e^{\left(\frac{\phi(x)-\phi_0}{k_B T_{es}}\right)} = n_{esmin}, \quad (2)$$

$$\phi_0 - \phi = \frac{k_B T_{es}}{e} \mathrm{Ln}\left(\frac{n_{e0}}{n_{esmin}}\right), \quad (3)$$

$\phi_0 - \phi$ is the value of the cut off.

Secondary emission yield (SEY) is the ratio between the emitted flux and the incident flux:

$$\delta = \frac{\gamma_{em}}{\gamma_{inc}} \propto \frac{n_{e0} v_{e0}}{\gamma_{inc}}, \quad (4)$$

with δ the SEY, γ_{em} the emitted flux of electrons, γ_{inc} the incident flux of electrons, and v_{e0} the velocity of emitted electrons. SEY varies from 1 at 30 eV incident electron energy to 2.1 at 200 eV, following an almost linear variation between these two energies [16]. The emission temperature of secondary electrons is 2 eV in this energy range [16,17]. Secondary electrons can not escape from the positive sheath and are attracted by the sample. They may create new secondary electrons (or they may be reflected). Few is known about low energy electron secondary emission yield, but the effective δ value is probably higher than expected. The incident electron flux γ_{inc} is constant for a given pressure and fixed by the electronic saturation current. Thus we can write

$$n_{e0} \propto \delta \quad (5)$$

and n_{e0} increases almost linearly with applied bias because of the linear increase of SEY with incident electron energy. Therefore the cut off value $\phi_0 - \phi$ increases as a logarithmic function of the applied bias:

$$\phi_0 - \phi = \frac{k_B T_e}{e} = \mathrm{Ln}\left(\frac{n_{e0}}{n_{esmin}}\right) = \frac{k_B T_e}{e} \mathrm{Ln}(A\phi_0 + B). \quad (6)$$

This behaviour of the cut off is qualitatively verified in Fig. 4.

The same result can be obtained considering radiative recombination phenomena close to surface. If we call $\Gamma_i(x)$ the ionization rate and $\Gamma_r(x)$ the radiative recombination rate, a decrease of the signal on the IEDF starts as soon as Γ_r becomes non negligible with respect to Γ_i (Fig. 2, decrease of the signal at 65 V). When Γ_r becomes higher than Γ_i too few ions can escape from the recombination zone to be detected and the cut off appears (Fig. 2 cut off at 9 V). If we call n_{esmin} the density of low energy electrons below which radiative recombination rate becomes negligible compared to the ionization rate, we can use exactly the same calculus (Eqs. (2)–(6)) to explain the cut off variation with bias voltage.

From the previous paragraphs, we can conclude that the observed phenomena is due to secondary electrons. However, we did not determine exactly how these secondary electrons induce it (shielding effect or ion–electron recombination effect). Therefore, absolute A and B values from Eq. (6) are not studied in the present paper. In the future we plan to model both effects to perform a full analysis of the phenomenon and obtain information from fit of Eq. (6) to experiments.

As plasma density, electronic saturation current increases with pressure. The Langmuir probe indicates that electronic saturation current goes from 18.8 mA m^{-2} for 0.05 Pa to 22.0 mA m^{-2} for 0.1 Pa. Thus, for each chosen bias the number of secondary electrons increases with pressure because of the increase of incident electron current (increase of γ_{inc}). As electron density locally increases, radiative recombination process is more efficient which

tends to increase the cut off with pressure. This could explain the increase of cut off with pressure observed in Fig. 4.

The local ionization rate in the sheath can be written as

$$\Gamma_i(x) = n_e(x)k_i(x)[\mathrm{Ar}] = n_e(x)v_e(x)\sigma(\varepsilon)[\mathrm{Ar}], \quad (7)$$

where n_e is the electron density (electrons from the plasma), k_i the ionization coefficient, [Ar] the neutral concentration, $v_e(x)$ the electron velocity, and $\sigma(\varepsilon)$ the ionization cross section with $\varepsilon = \phi(x) - \phi_p$ (ϕ_p is the plasma potential). Electron current ($n_e(x)v_e(x)$) is conserved inside the sheath and one can see that ionization rate should follow the ionization cross section. Fig. 2 shows a 'triangular' shape of the measured IEDF at 70 V. This 'triangular' shape is only obtained at low bias. Plasma potential for this pressure is 36 V. Therefore electrons are accelerated across a potential of 34 eV ($\phi_0 - \phi_p$). In this energy range, ionization cross section strongly increases. Therefore ionization rate increases along the sheath explaining the increase of the IEDF intensity with energy. Since total electronic ionization cross section little varies in the energy range of 60–110 eV [15], we obtain an almost constant IEDF intensity over the energy range scanned as soon as the bias is raised to 110 V (Fig. 3).

5. Conclusion

We presented ion energy measurements by means of a Hiden EQP300. By analyzing the behaviour of ion creation in a positive sheath between plasma and a positively biased sample, we showed existence of an electron gas due to secondary electron emission. In the first approximation the potential profile follows a Child–Langmuir law. However, curvature of the sheath potential due to secondary electrons and radiative recombination close to the sample could explain the very weak density of high energy ions on the IEDF. Results are well correlated with sample surface characteristics, in particular with its secondary electron emission yield (SEY). In the future, we plan to develop a modelling of the potential profile within the sheath, to take into account potential curvature profile induced by secondary electrons close to surface. Once this effect will be quantified, we plan to study other sample materials, like graphite, in argon or in hydrogen plasmas. Concerning material, we expect to have different cut off values depending on graphite SEY and secondary electron temperatures. Concerning gas, the main difference will be the presence of multiple ions (H^+, H_2^+, H_3^+ in H_2 plasma).

Acknowledgements

The authors thank Dr R. Boswell, Dr N. Sadeghi and Dr P. Brault for all the stimulating discussions and many helpful suggestions. This work was supported by the 'Fonds Europeéns de Developpement Et de Recherche', CNRS, 'Conseil Général 13', CEA, the University of Provence.

References

[1] F. Gaboriau, G. Cartry, M.C. Peignon, Ch. Cardinaud, J. Vac. Sci. Technol. B 20 (4) (2002) 1514.
[2] S. Qin, Surf. Coat. Technol. 86 (1996) 56.
[3] S. Radovanov, L. Godet, R. Dorai, Z. Fang, B.W. Koo, C. Cardinaud, G. Cartry, D. Lenoble, A. Grouillet, J. Appl. Phys. 98 (113307) (2005) 1514.
[4] P. Degond et al., C.R. Acad. Sci. Paris, Ser. I 335 (2002) 399.
[5] L. Yongdong, W. Hongguang, L. Chunliang, S. Jian, Appl. Surf. Sci. 251 (2005) 19.
[6] J.W. Bradley, G. Lister, Plasma Source Sci. Technol. 6 (1997) 524.
[7] A. Anders, Surf. Coat. Technol. 136 (2001) 85.
[8] Naoufel Ben Abdallah et al., Solid State Electron. 39 (5) (1996) 737.
[9] Naoufel Ben Abdallah et al., Nonlinear Anal. Theory Meth. Appl. 31 (5–6) (1998) 629.
[10] Y. Miyagawa, M. Ikeyama, S. Miyagawa, H. Nakadate, Nucl. Instrum. and Meth. B 206 (2003) 767.
[11] G. Rangelov, V. Dose, Surf. Sci. 395 (1998) 1.
[12] V. Kaeppelin, M. Carrère, J.B. Faure, Rev. Sci. Instrum. 72 (12) (2001) 4377.
[13] A.V. Phelps, J. Phys. Chem. Ref. Data 20 (3) (1991) 557.
[14] H.C. Straub, P. Renault, B.G. Lindsay, K.A. Smith, R.F. Stebbings, Phys. Rev. A 52 (1995) 1115.
[15] H. Tawara, M. Kato, National Institute for Fusion Science, NIFS Data 51, 1999.
[16] M.A. Furman, M.T.F. Pivi, Phys. Rev. – Accelerators and Beams 5 (2002) 124404.
[17] V. Baglin, I. Collins, B. Henrist, N. Hilleret, G. Vorlaufer, LHC Project Report 472, 2002.